Hindawi
Advances in Civil Engineering
Volume 2020, Article ID 5242406, 14 pages
https://doi.org/10.1155/2020/5242406

Research Article

The Study on Early-Age Expansion and Shrinkage Model of Massive Self-Compacting Concrete Pumped in Steel Tube Column

Zhen-jun He,[1] **Meng-jia Ding**,[2] **Zhen-wei Wang**,[1] **Xue-sheng Zhang**,[3] **Mei-gen Cao**,[1] **and Ming-wei Lei**[4]

[1]*School of Civil Engineering, North China University of Technology, Beijing 100144, China*
[2]*College of Architecture and Civil Engineering, Beijing University of Technology, Beijing 100124, China*
[3]*Beijing Urban Construction Group Co., Ltd., Beijing 100016, China*
[4]*China Xinxing Construction and Development Co., Ltd., Beijing 100039, China*

Correspondence should be addressed to Zhen-jun He; zjhe@ncut.edu.cn

Received 24 December 2019; Revised 28 April 2020; Accepted 17 August 2020; Published 15 September 2020

Academic Editor: Gang Zhou

Massive self-compacting concrete pumped in steel tube columns has been used more and more widely in super high-rise buildings and bridge engineering at present. The early-age expansion and shrinkage performance of its core mass concrete is an important index to ensure the stress state of triaxial compression and structural safety. However, no relevant reports have been found. In view of the actual building with the height of 265.15 meters, the early-age expansion and shrinkage tests of the massive self-compacting concrete pumped in full-scale columns with the height of 12.54 m and 12.24 m and diameter of 1.3 m and 1.6 m were carried out by means of strain gauges embedded in concrete-filled steel tubes (CFSTs). The early-age variation regularity of the vertical and horizontal expansion and shrinkage strains for the core concrete with the diameter of steel tube, development time, temperature, the pouring pressure, expansion stress, and so on is given. The calculation model of its early-age deformation strains is presented in this paper, which is in good agreement with the experimental results. It provides the basis of experimental and theoretical analyses for shrinkage compensation of massive self-compacting concrete pumped in steel tube columns.

1. Introduction

As a composite component of steel and concrete, it must be ensured that its core concrete of concrete-filled steel tube (CFST) is in a complex stress state under three-dimensional compression and there is the rigid restraint effect for the core concrete formed in the steel tube, so as to improve the compressive strength and deformation capacity of the core concrete, promote the improvement of its plasticity and toughness, and prevent the brittle failure of the core concrete in steel tube. Therefore, the characteristics and changing regularity of the early-age expansion and shrinkage deformation for the core concrete are particularly important, which is the premise to ensure both works together. At present, the research on shrinkage and expansion properties of CFST at home and abroad is as follows.

Yang et al. [1] stated that the concrete shrinkage and creep strains in recycled aggregate concrete-filled steel tubes (RACFST) specimens were about 6% to 23% higher than those of the corresponding normal CFST specimens. Results obtained by Abdalhmid et al. [2] showed that FA reduced the rate of hydration and thus the drying shrinkage of self-compacting concrete (SCC) containing fly ash (FA) was considerably lower than that of the control concrete. Yan et al. [3] reported that the quantity of ettringite was a very critical factor in determining the expansion of mortars, but mortar structure, morphology of ettringite, and curing humidity were also relevant. Gonzalez-Corominas and Etxeberria [4] found that the plastic shrinkage of concretes increased as the employed recycled concrete aggregates (RCA) quality was reduced and the replacement ratio was increased. However, the obtained values for all high-performance concrete (HPC) concretes were lower than those

required with respect to concrete cracking. The results of Oliveira et al. [5] also showed that the curing time was essential to minimize shrinkage at early ages. It caused a lower drying mass loss causing a delaying effect in the development of shrinkage. This was important for early cracking proneness. The study of Gribniak et al. [6] dealt with concrete shrinkage and accompanying creep influence on cracking resistance and deformations of structural elements. It was found that serviceability characteristics of reinforced concrete elements at the design stage might be improved by specifying (1) concrete mixture proportions; (2) mechanical properties of aggregates; (3) method of curing; (4) ambient temperature and humidity conditions; and (5) geometry of the structural element. It was found that the autogenous shrinkage of early-age high-performance concrete (HPC) under different curing temperatures could not be predicted by the singular application of the equivalent age concept. The possible reason was that the microstructure evolution and apparent activation energy were influenced by temperature. Thus, investigation on the effect of curing temperature on cracking resistance of early-age concrete must be further studied [7]. The general trends [8] observed indicated that the American Association of State Highway and Transportation Officials (AASHTO) method tended to overpredict shrinkage for both concrete mixtures, especially at early ages, and no method accurately represented the lower shrinkage rate of lightweight self-consolidating concrete (LWSCC). Benboudjema et al. [9] pointed out that the drying process caused a strong structural effect: microcracking arises in the concrete skin and attenuates the free drying shrinkage strain. The amplitude of the structural strain was quite large. It highlighted the need for an adequate cracking model to separate accurately the intrinsic behavior of the material from the structural induced effect. Nevertheless, after one year, the numerical curve deviated from the experimental one. This behavior seemed to be intrinsic, since the adopted mechanical model took into account most of the characteristics of cracked concrete. The experimental results of Wu et al. [10] showed that internal curing was an effective means to reduce the autogenous shrinkage of high-performance concrete. The results of Persson [11] indicated that carbonation shrinkage may be avoided by the addition of silica fume. Xie et al. [12] suggested that, from the perspective of reducing shrinkage, the optimal binder-to-sand ratio was in the range of 1–1.1; the optimal dosage rate of shrinkage reducing admixture was 1%; and replacing of mixing water by crushed ice up to 50% by weight had also induced a significant reduction in shrinkage. Wang et al. [13] suggested that the incorporation of 10-Mas. % expansive agent was useful to diminish the shrinkage, especially by its combined use with prewetted lightweight aggregates (PLWA). The results of Oliveira et al. [14] also showed a potential for achieving a predefined shrinkage range, by using the combined effect of a set retarder and an expansive admixture. The paper [15] presented the main results of a research carried out to analyze the mechanical properties, intrinsic permeability, drying shrinkage, carbonation, and the self-healing potential of concrete incorporating recycled concrete aggregates. However, the effect of curing temperature on autogenous shrinkage of early-age concrete was not in consistency and how the curing temperature affected the cracking resistance of concrete remains lacking. Analysis of shrinkage stresses of concrete-filled steel tube (CFST) arch bridges showed that the shrinkage self-stress was large and should be taken into account in design calculation [16]. The results of Cao et al. [17] indicated that the shrinkage strain of a concrete-filled steel tube was mainly caused by self-shrinkage, and the self-shrinkage strain was about 1×10^{-4}. Zhu et al. [18] reported that the shrinkage of a concrete-filled steel tube can be compensated well when the amount of expansive agent was 12%. Chen [19] found that the strains of free shrinkage and limited shrinkage were 407×10^{-6} and 137×10^{-6}, respectively, at fourteen days.

For the massive self-compacting concrete pumped in steel tube column, the expansion and shrinkage of the core concrete affects the stress distribution of concrete-filled steel tubular members to a great extent, which can produce redistribution of internal stress in concrete-filled steel tubular members, including "redistribution of internal stress in the section and internal stress in the system." For example, during the shrinkage process of the core concrete in CFST, the steel tube is forced to participate in the work alone, resulting in tensile stress in the core concrete and compressive stress in the steel tube, resulting in redistribution of the internal stress in the section, and the distribution values are large. Besides, when the core concrete shrinks, there is a gap between the core concrete and the steel tube, which not only destroys the joint work between the steel tube and the core concrete but also may cause corrosion on the inner surface of the steel tube during use. In addition, the excessive expansion of the core massive concrete in the steel tube will cause serious damage to the steel tube, thus making the structure in an unsafe state.

Based on the above, the early-age shrinkage and expansion properties for the massive self-compacting concrete pumped in steel columns have been studied in this paper.

2. Materials and Experimental Procedures

2.1. Materials and Mix Proportions. The cementitious materials used for this investigation were Chinese standard P·I42.5R Portland cement (standard compressive strength higher than 42.5 MPa at the age of 28 days), Class I fly ash (fineness of 45 μm not more than 12%, water demand ratio not greater than 95%, and loss on ignition not more than 5%), and silica fume (the National Standards of the People's Republic of China for Portland Cement and Ordinary Portland Cement, 1999; Fly Ash Used for Cement and Concrete, 2005; Silica Fume for Cement Mortar and Concrete, 2012). The coarse aggregate was a natural crushed stone (diameter 5–20 mm); the fine aggregate was natural river sand (fineness modulus of 2.7); and tap water was used for mixing. Tables 1 and 2, respectively, show the mix proportions by weight of the mixture and the major parameters of massive self-compaction concrete pumped in steel tube columns.

Table 1: Mix proportions of massive self-compacting concrete pumped in steel tube columns.

Strength grade	Water/ binder ratio	Water (kg/m^3)	Cement (kg/m^3)	Fly ash (kg/m^3)	Silica fume (kg/m^3)	Fine aggregate (kg/m^3)	Coarse aggregate (kg/m^3)	Superplasticizer (kg/m^3)
C60	0.31	165	320	180	25	790	850	8.6

Table 2: Major parameters of massive self-compacting concrete pumped in steel tube columns.

Mixture performance (1 hour after the concrete is discharged from the mixer)				Compressive strength/ MPa				Dry shrinkage/$\times 10^{-6}$ m/m						
Air contents	Slump	Slump flow	V-shaped funnel test	3 d	7 d	28 d	60 d	3 d	7 d	14 d	28 d	60 d	90 d	180 d
3.2%	255 mm	700 mm	14 s	39.5	54.8	78.9	86.7	−79	−176	−237	−305	−378	−412	−431

2.2. Samples and Testing Methods

2.2.1. Casting Method of Pumped Concrete. The maximum outlet pressure of HBT105.21.280RS concrete pump with high reliability was designed to be 21 MPa, and the pressure reserve was 13.3%. The pumping rates were 35–45 m^3/h. In order to facilitate the removal of gas in the steel tubes, it was necessary to open 4Φ20 mm vent holes on the wall of steel tubes by every 1.5–2 m along the length of the column. Test columns and their dimensions are shown in Figures 1 and 2.

Figure 1: Test columns.

2.2.2. Apparatus and Testing Methods. The vertical and horizontal expansion and shrinkage deformation of massive self-compacting concrete pumped in the core concrete of CFST were measured by the embedded strain gauges. The arrangement of the strain gauges of measurement points is shown in Figure 3. Two pairs of large volume strain gauges embedded in CFST were symmetrically arranged inside each CFST column. The arrangement distance between the horizontal position of the strain gauges and the top of the CFST column was 650 mm, and the vertical and horizontal spacing of the four embedded strain gauges were $D/4$ of the diameter, which were 325 mm and 400 mm, respectively, as shown in Figure 3. Notes: the first number of "1–1" stands for the SYZ-1 test column; the second number of "1–1" stands for the first measuring point.

BGK-4210 embedded strain gauges with a standard distance of 250 mm were adopted, which was suitable for strain measurement of massive concrete. A total of eight gauges for both CFST columns were needed. We ensured that the embedded strain gauges were geometrically aligned and placed horizontally. After the strain gauges and other devices were installed, it was necessary to calibrate them before the core concrete was poured. The early-age expansion and shrinkage deformation were collected regularly and continuously every day.

Wzp-pt100 armored platinum thermal resistance was used in the temperature test. In consideration of the symmetry of the test column, the temperature test section was taken as one-half of the diameter for testing. In addition to ensuring the thermal resistance required by the measuring point of the internal temperature of the core concrete, a temperature instrument was also set up to measure the temperature inside and outside the test shed. The specific layout of 1 to 6 measuring points is shown in Figure 3. Measuring point 5 corresponded to the temperature in the test shed, and measuring point 6 corresponded to the outdoor temperature. The test duration of this hydration heat temperature was 28 days. The collection interval was 1 minute by 24-hour continuous collection. When dealing with data results, data points were selected according to the required time interval.

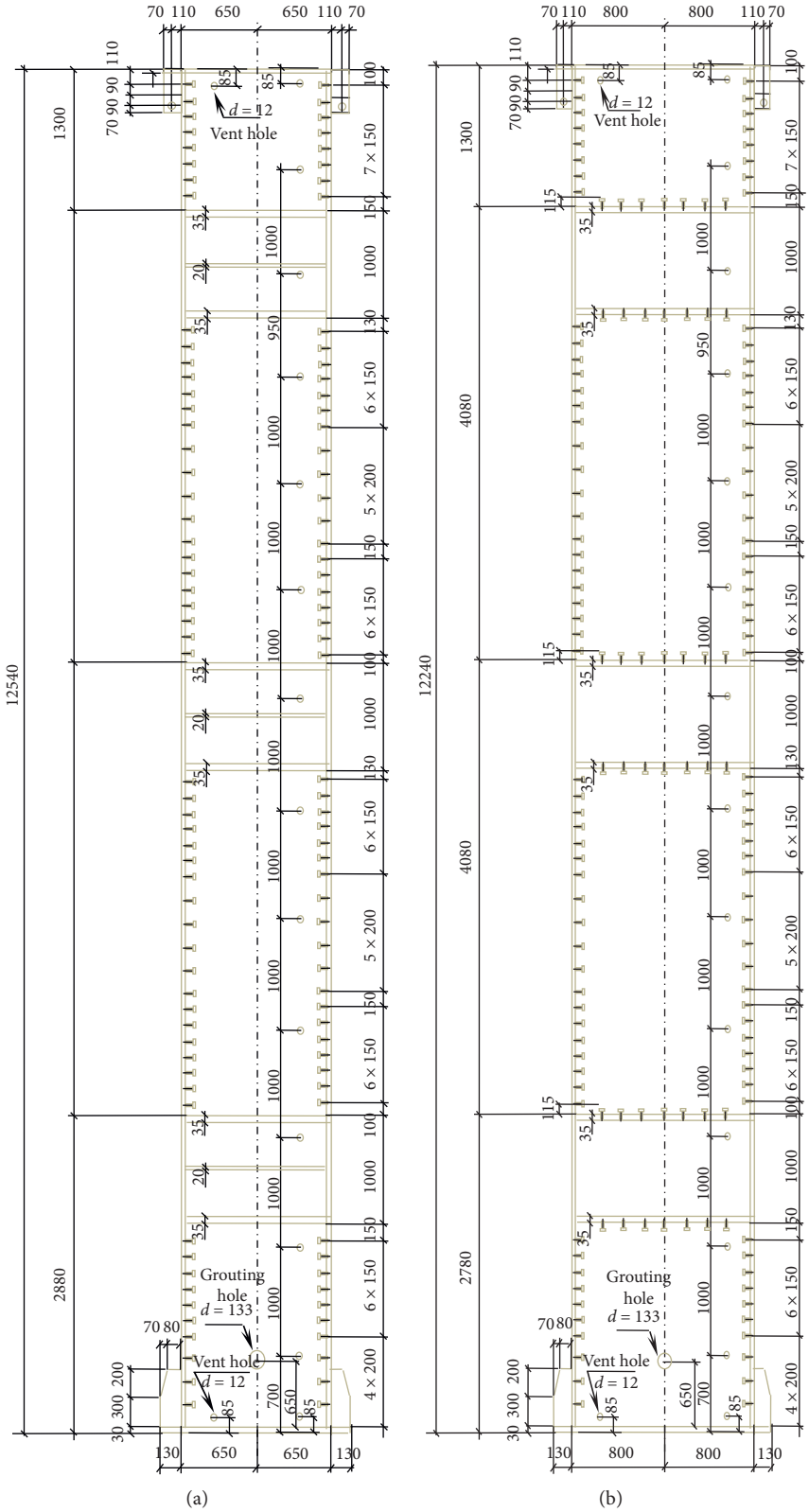

Figure 2: Design drawings of CFST columns used in engineering (unit: mm). (a) SYZ-1 test column. (b) SYZ-2 test column.

BGK-4810 vibrating concrete pressure cells were used in the test of the pouring pressure and expansion stress of the core concrete. Four pressure cells were arranged for SYZ-1 column with the height of 940 mm, 4470 mm, 8650 mm, and 11890 mm, respectively; three pressure cells were arranged for SYZ-2 column with the height of 2280 mm, 6360 mm,

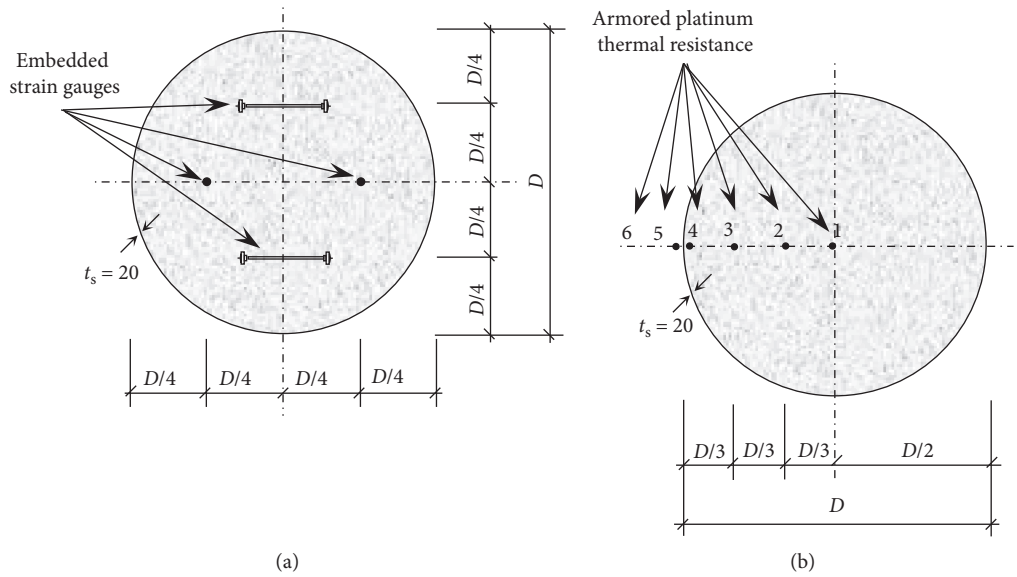

Figure 3: Arrangement drawings of test instruments for cross section of column (unit: mm). (a) Layout of deformation measurement points. (b) Layout of temperature measurement points.

and 10440 mm, respectively. Each height corresponded to 1~4 measuring points, respectively. Figures 4 and 5 show actual arrangement installation photos of the test instruments and equipment.

3. Test Results and Analysis

3.1. Change Laws between Temperature and Development Time. As shown in Figure 6, the relationship between the measured hydration heat temperature (T) in the cement hydration stage of the core concrete for the CFST test column and development time (t) is given. It can be seen from Figure 6 that when the daily outdoor temperature reached the maximum values, the temperature curve of 1 to 4 measuring point shows a slightly rising inflection point, which is the most obvious near the temperature measuring points 3 and 4 of the steel tube wall; that is to say, the hydration rates are greater than those of the heat dissipation at this time, and the higher the daily outdoor temperature is, the larger the increasing extent of curve is. It can also be seen from Figure 6 that, with the increase of hydration time, the temperature difference of each measuring point gradually decreases and finally tends to be the same. This is because the hydration process for each measuring point of the core concrete has basically tended to be the same. At the same time, with the increase of time, the temperature of each measuring point gradually tends to the temperature in the test shed.

As shown in Figure 6, the temperature of each measuring point for the core concrete of the test column rises rapidly first, because the temperature values of the poured concrete itself are higher than those in the test shed. Then, it decreases slightly, just because there is a temperature difference between the temperature of the poured concrete into the mold and the temperature in the test shed, and there is heat transfer between them. At this time, the hydration heat has not been formed to offset this heat loss, resulting in a slight drop in the temperature of the core concrete itself. The release amount of cement hydration heat does not increase until about 10 hours after pouring concrete, and it rises slowly and continuously. At this time, the rates of hydration heat are greater than those of heat dissipation. When the hydration heat rates and heat dissipation rates reach the balance, the section temperatures of the test columns reach the peak value for about 38 hours after pouring. Then, they continue to decline until it approaches to the temperature in the test shed.

It can be seen from Table 3 and Figure 6 that the peak values of temperature at measuring points 1~4 of SYZ-1 test column were 33.7°C, 32.6°C, 27.9°C, and 22.3°C, respectively. The peak values of temperature at measuring points 1~4 for SYZ-2 test column were 39.1°C, 36.6°C, 29.0°C, and 19.6°C, respectively. During the test of hydration heat temperature after pouring concrete, with the increase of time, the temperature range in the test shed was −8.9~10.9°C, and the outdoor temperature range was −10.9~11.5°C. The measured curve in Figure 6 shows that, in the initial stage of pouring concrete, the temperature distribution of the cross section generally reflects the law that was high in the internal parts and low in the external parts, and the temperature difference between the center and the outer edge of the section was bigger. This is because concrete is a kind of material with low thermal conductivity, and it is not easy to dissipate the large amount of hydration heat produced by cement hydration. Thus, the temperature difference was formed along the diameter direction of the test column, resulting in different temperature values of measuring points 1–4. The maximum value of temperature difference between the center of the core concrete and its outer edge was about 5°C. In the initial stages of pouring concrete, the temperature section values of the test column were significantly higher than those of the outdoor temperature, and the maximum value of

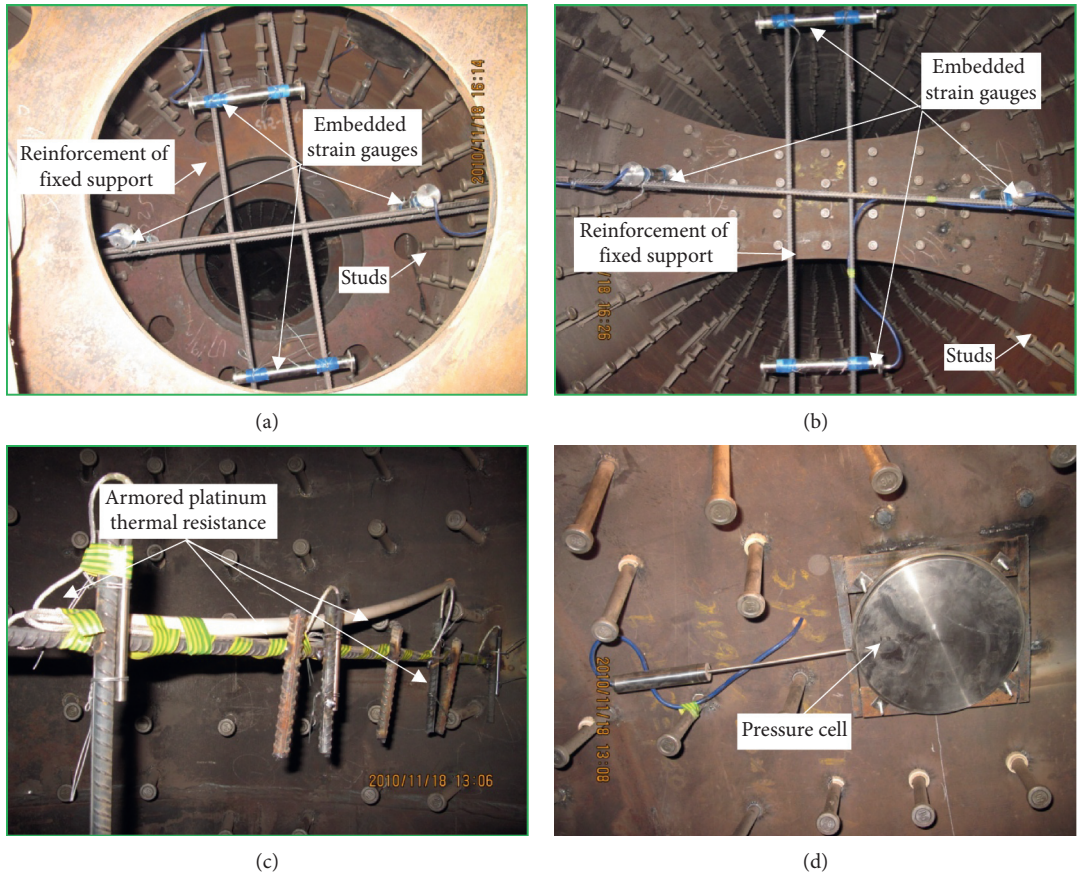

Figure 4: Arrangement photos of test instruments. (a) Deformation measurement of SYZ-1 column. (b) Deformation measurement of SYZ-2 column. (c) Temperature measurement. (d) Vibrating-wire pressure cell.

temperature difference between the section center and the outdoor temperature was 18°C.

Based on the above analysis, temperature parameters must be included in the early-age expansion and shrinkage model of massive self-compaction concrete pumped in steel tube column.

3.2. Change Laws between the Pouring Pressure and Expansion Stress and Development Time. Figures 7 and 8, respectively, show the relationship between the pouring pressure and expansion stress of the core concrete for SYZ-1 and SYZ-2 column and development time. As can be seen from Figures 7(a) and 8(a), the pouring pressure reached the maximum after pouring; then, as the core concrete gradually solidified, its pressure gradually decreased. For each measuring point, the platform stage before the curve reaches the peak value is the waiting period of pouring concrete; if there is no waiting time for pouring concrete, the curve shows continuity, and the curve does not display the landing steps.

It can be seen from Figures 7(b) and 8(b) that, for SYZ-1 column, the compressive stress on the inner wall of steel tube increases gradually for nearly 19 hours after pouring, and four measuring points reach the maximum peak expansion stress for about 32 hours after pouring. For SYZ-2 column, the pressure gradually increased for nearly 20 hours after pouring, and the maximum peak expansion stress was reached at three measuring points for about 39 hours after pouring. It can be seen from Table 4 and Figures 7(b) and 8(b) that the peak value of pouring pressure at measuring points 1~4 for SYZ-1 column is 0.025 MPa, 0.094 MPa, 0.197 MPa, and 0.283 MPa, respectively. The peak value of expansion stress at measuring points 1~4 for SYZ-1 column is 0.407 MPa, 0.505 MPa, 0.53 MPa, and 0.37 MPa, respectively. The peak value of pouring pressure at measuring points 1~3 for SYZ-2 column is 0.208 MPa, 0.282 MPa, and 0.37 MPa, respectively. The peak value of expansion stress at 1~3 measuring points for SYZ-2 column is 0.657 MPa, 0.712 MPa, and 0.686 MPa, respectively. From the above test results, it can be seen that the pouring pressure is not great, which will not cause harm to the steel tube wall, but the pouring pressure at the joint of the through center plate is greater than that of other nonjoint; in addition, the larger the cross-section size of the steel tube column, the greater the expansion stress and the later the time when it reaches the peak expansion stress.

From Figures 7(c) and 8(c), it can be seen that, for SYZ-1 column, the pressure of four measuring points basically tends to be stable in about 3 days after pouring; for SYZ-2 column, the pressure of three measuring points basically tends to zero in about 15 days after pouring; and after that, the core concrete forms tensile stress on the inner wall of the steel tube, reaching the maximum 0.15 MPa tensile stress in about 20 days, and then tends to zero. The reason is that

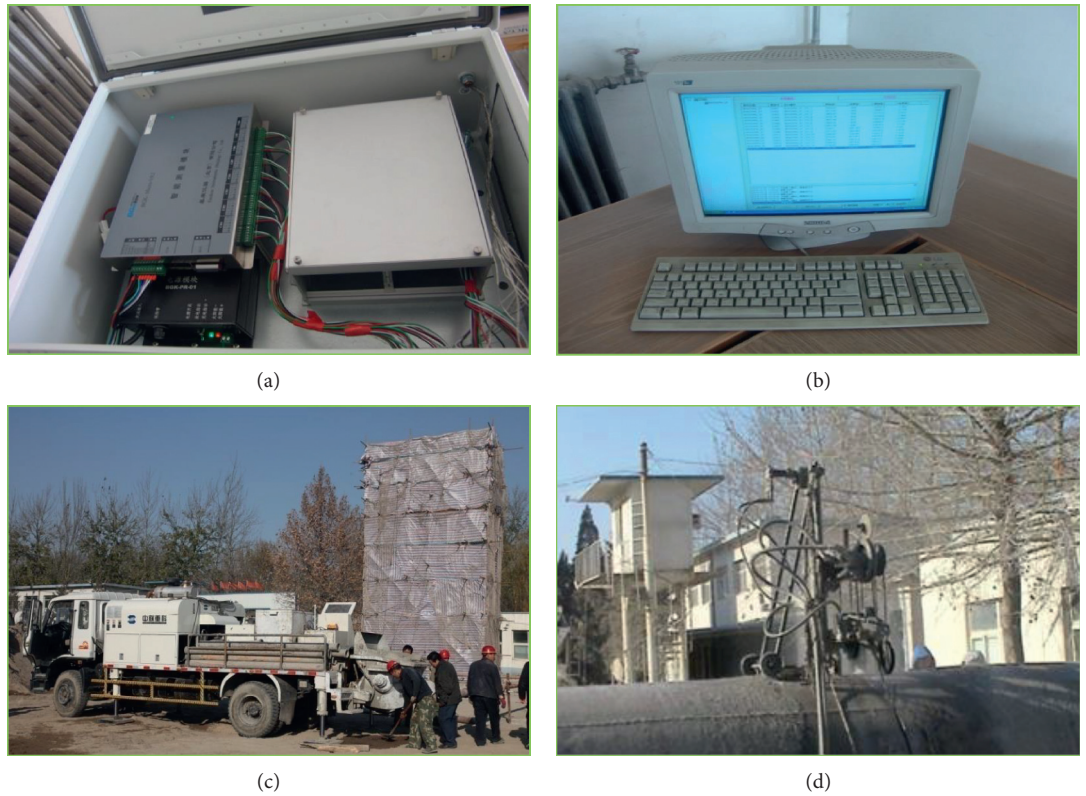

Figure 5: Test equipment. (a) Data collection instrument for vibrating-wire sensor. (b) Data collection computer. (c) Concrete pump truck. (d) Wire saw for cutting.

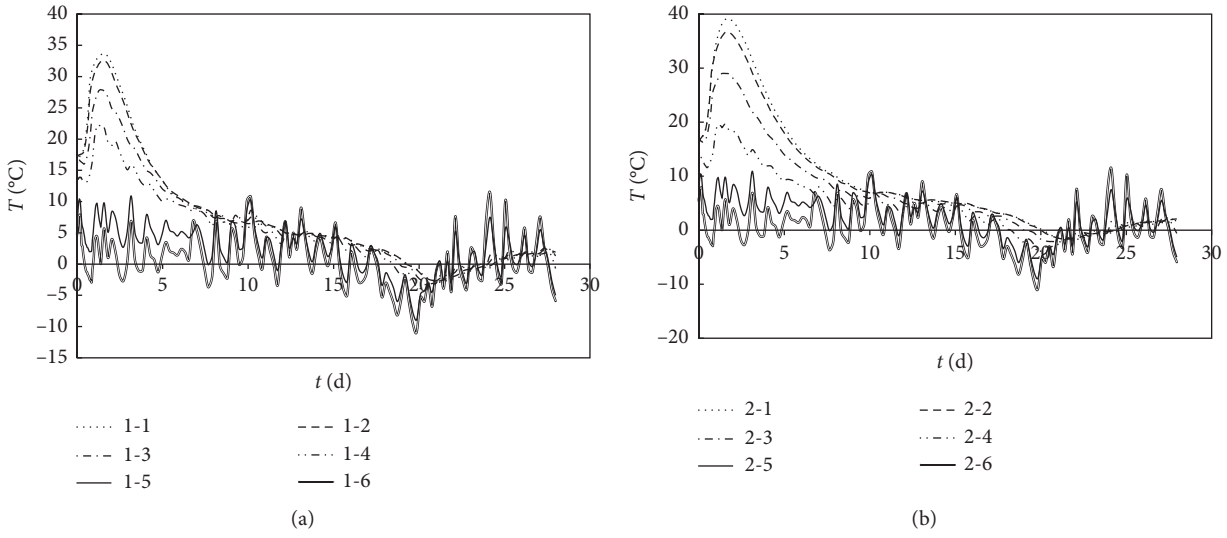

Figure 6: Test curves of temperature measurement of the core concrete. (a) SYZ-1 column. (b) SYZ-2 column.

there is a certain adhesive force between the surface of the pressure cell and the core concrete, and the additional internal force generated by the shrinkage deformation of the core concrete drives the steel pipe, which shows a certain amount of tensile stress. Therefore, it can be seen that the shrinkage of the above SYZ-2 column in the joint area is greater than that in the nonjoint area.

3.3. Change Laws between the Vertical and Horizontal Strains and Development Time. Figure 9 shows the relationship between the vertical and horizontal strains of the measured deformation and development time. From Figure 9, it can be seen that the vertical and horizontal strains of the measured deformation of the core concrete in CFST columns similarly change with development time. The early-age strains of the

Table 3: Maximum values of temperature at each measuring point of the core concrete.

Type of steel tube column	Measuring points					
	1	2	3	4	5	6
SYZ-1	33.7°C	32.6°C	27.9°C	22.3°C	10.9°C	11.5°C
SYZ-2	39.1°C	36.6°C	29.0°C	19.6°C		

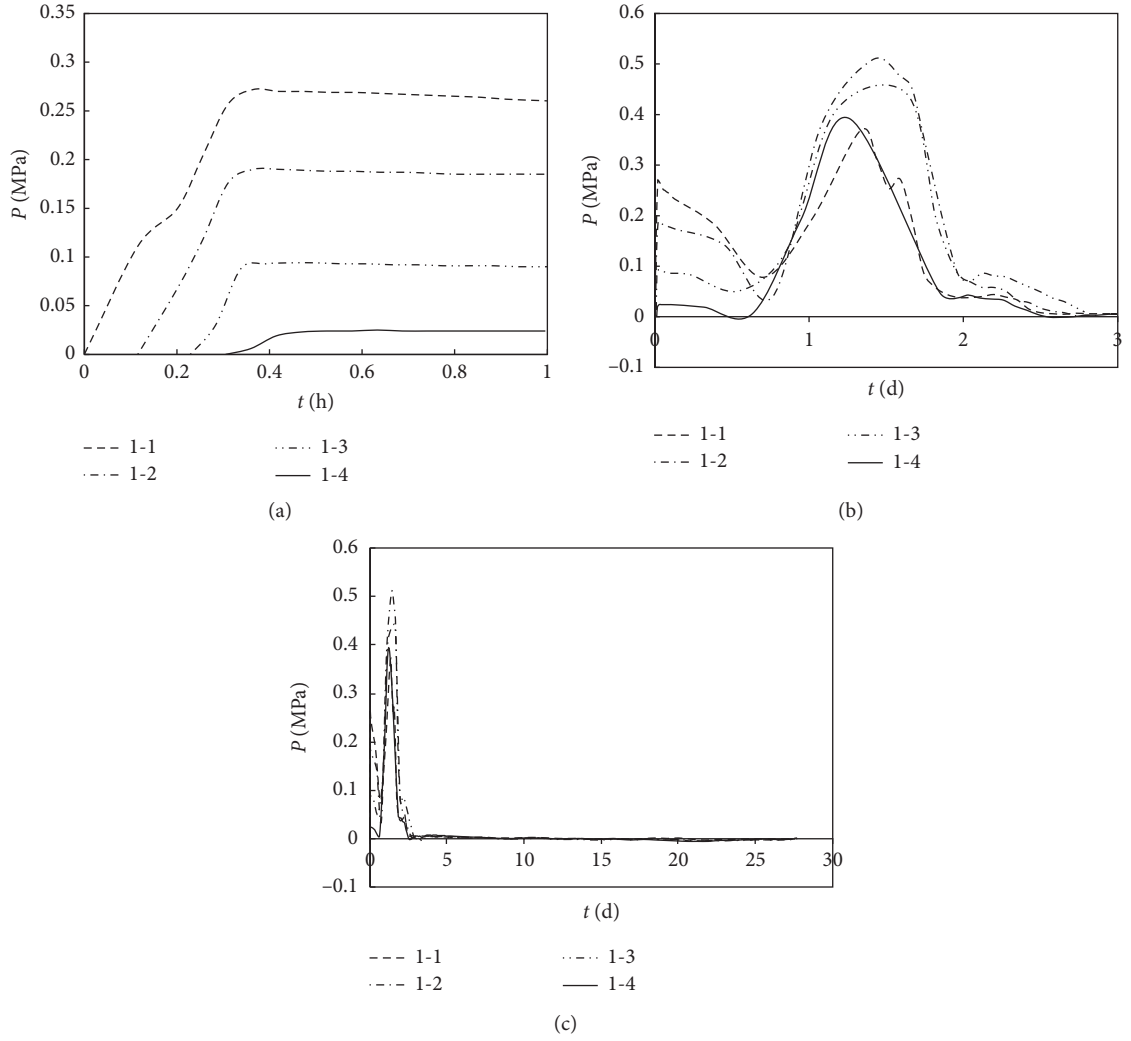

Figure 7: Test curves of pouring pressure and expansion stress of the core concrete for SYZ-1. (a) 1 hour. (b) 3 days. (c) 28 days.

core concrete develop rapidly. Its expansion strains first occur, and then there are shrinkage strains. The expansion strains occur within 2.5 days after the core concrete was poured. The curves of shrinkage strain for both CFST columns show a significant turning point around the 9th day after pouring. The curves change slowly over time and reach the peak of shrinkage strains around the 21st day, and then the curves flatten.

It can be seen from Table 5 and Figure 9 that, for SYZ-1 column, the values of the vertical and horizontal expansion strains are 30.295 $\mu\varepsilon$ and 23.792 $\mu\varepsilon$, 70.58 $\mu\varepsilon$, and 87.019 $\mu\varepsilon$, respectively. For SYZ-2 column, the values of the vertical and horizontal expansion strains are 6.824 $\mu\varepsilon$ and 8.777 $\mu\varepsilon$, 31.654 $\mu\varepsilon$, and 38.513 $\mu\varepsilon$, respectively. The values of the horizontal expansion strains are greater than those of the vertical ones. The values of the two kinds of expansion strains for a small diameter of CFST are greater than those of large diameter ones.

For SYZ-1 column, the maximum values of the vertical and horizontal strains for early-age shrinkage of the core concrete in 28 days are −414.518 $\mu\varepsilon$ and −402.06 $\mu\varepsilon$, −365.37 $\mu\varepsilon$, and −335.686 $\mu\varepsilon$, respectively; for SYZ-2 column, the maximum values of the vertical and horizontal strains for it are −323.532 $\mu\varepsilon$ and −302.18 $\mu\varepsilon$, 268.006 $\mu\varepsilon$, and −269.299 $\mu\varepsilon$, respectively, which are much greater than those of the two kinds of cross-section sizes in [20]; that is, vertical and horizontal shrinkage values for square steel tubes of 200 × 200 mm (102.1 $\mu\varepsilon$ and 91.5 $\mu\varepsilon$) and

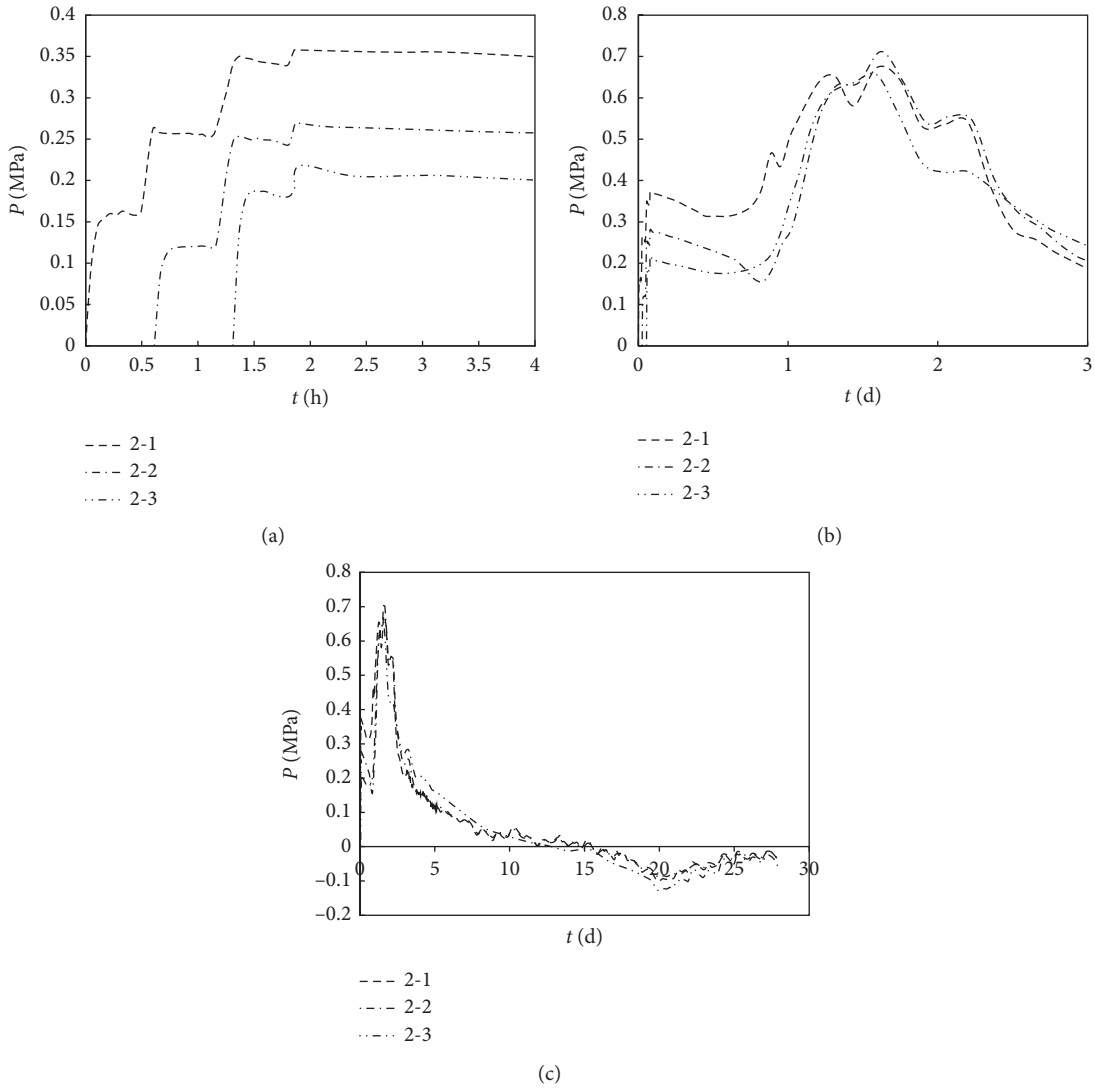

Figure 8: Test curves of pouring pressure and expansion stress of the core concrete for SYZ-2. (a) 4 hours. (b) 3 days. (c) 28 days.

Table 4: Maximum values of pouring pressure and expansion stress at each measuring point of the core concrete.

Type of steel tube column	Types of force	Measuring points			
		1	2	3	4
SYZ-1	Pouring pressure	0.025 MPa	0.094 MPa	0.197 MPa	0.283 MPa
	Expansion stress	0.407 MPa	0.505 MPa	0.530 MPa	0.370 MPa
SYZ-2	Pouring pressure	0.208 MPa	0.282 MPa	0.370 MPa	—
	Expansion stress	0.657 MPa	0.712 MPa	0.686 MPa	—

1000×1000 mm (47.2 $\mu\varepsilon$ and 30.4 $\mu\varepsilon$) were calculated. The values of the vertical strains for early-age shrinkage are greater than those of the horizontal ones. The values of the two kinds of shrinkage strains of the core concrete for small diameter CFST are greater than those of large diameter ones.

Through the analysis of the above experimental results, it can be concluded that, for SYZ-1 column, the difference values between vertical and horizontal shrinkage deformation are not significant in the first 6 days, but for SYZ-2 column, there was slightly greater difference for the above, and the difference values tend to increase with the change of time. For the CFST column of the same diameter size, the values of the vertical shrinkage strains are much greater than those of the horizontal shrinkage strains at the same time, which may be due to the influence of the self-weight of concrete and spatial effect on the vertical shrinkage of the core concrete.

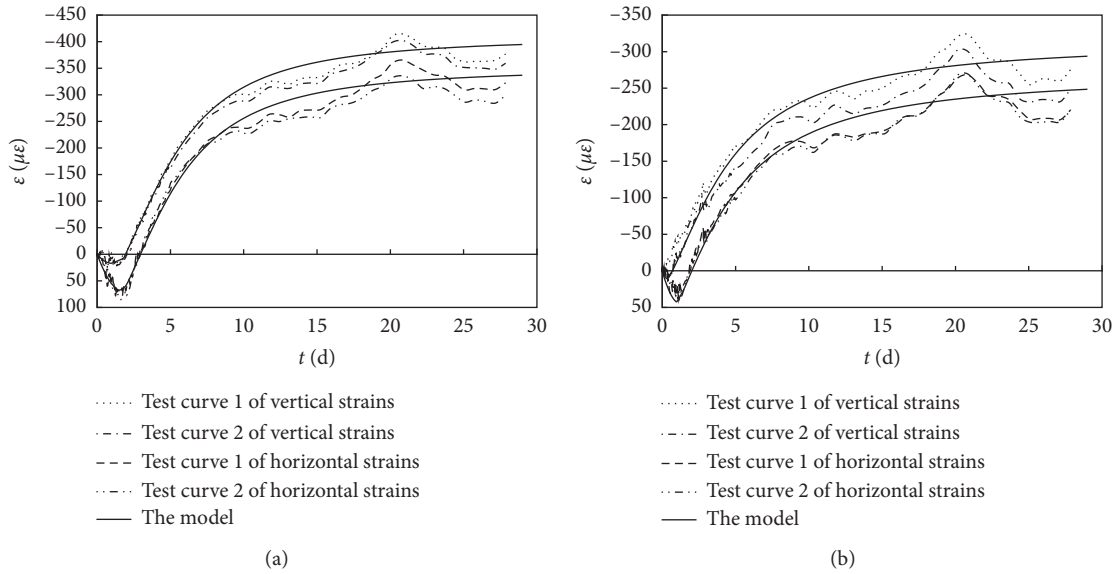

Figure 9: Comparisons between the calculation model and test curves. (a) SYZ-1 column. (b) SYZ-2 column.

Table 5: Maximum values of expansion and shrinkage strains of the core concrete.

Type of steel tube column	Expansion and shrinkage directions	Expansion strains	Shrinkage strains
SYZ-1	Vertical	30.295 $\mu\varepsilon$	−414.518 $\mu\varepsilon$
		23.792 $\mu\varepsilon$	−402.060 $\mu\varepsilon$
	Horizontal	70.580 $\mu\varepsilon$	−365.370 $\mu\varepsilon$
		87.019 $\mu\varepsilon$	−335.686 $\mu\varepsilon$
SYZ-2	Vertical	6.824 $\mu\varepsilon$	−323.532 $\mu\varepsilon$
		8.777 $\mu\varepsilon$	−302.180 $\mu\varepsilon$
	Horizontal	31.654 $\mu\varepsilon$	−268.006 $\mu\varepsilon$
		38.513 $\mu\varepsilon$	−269.299 $\mu\varepsilon$

Therefore, the development trends of the horizontal and vertical shrinkage deformation show some differences. The values of the horizontal strains of temperature expansion are greater than those of its vertical ones at the same time, which is the main reason for the change caused by different spatial constraints. The values of the vertical and horizontal shrinkage strains of temperature expansion for small diameter CFST columns are greater than those of large diameter ones at the same time.

Based on the experimental measurement of hydration heat temperature, expansion pressure, expansion, and shrinkage strain of the core concrete and through theoretical analysis, the interaction mechanism of the above three aspects is as follows: at the initial stage of mass concrete pouring, a large amount of hydration heat is released from cement hydration reaction, which quickly accumulates in the concrete, making the concrete temperature rise and the expansion volume of concrete increase. Temperature stress and temperature difference stress will be generated, and their numerical sizes also involve many factors such as the plane size of the structure, structure thickness, constraints, characteristics of various composite materials of concrete, physical and mechanical properties, and construction technology; with the release of heat and the end of heat exchange with the environment, the temperature of concrete decreases, and the volume of concrete shrinks. When the shrinkage is constrained, tensile stress occurs. At this time, the newly poured concrete, no matter its tensile strength and force which are very small, is not enough to resist the tensile stress, so cracks appear in its concrete.

4. Calculation Model of Early-Age Expansion and Shrinkage Deformation

Based on the analysis for the experimental results in this paper and the existing shrinkage models of concrete at home and abroad [20–22] and in view of the fact that the core concrete is sealed in steel tube, the variation law of its relative humidity is different from the general situation. Therefore, based on the above comparison and consideration, the calculation model proposed in this paper on the early-age expansion and shrinkage for the massive self-compacting concrete pumped in steel tubes has the following characteristics:

(1) The formula for the calculation model incorporates factors such as the limit shrinkage strain (ε_{shu}) of the core concrete in standard state, the time-development function ($\beta(t)$) of the early-age expansion and shrinkage, and the correction coefficients of various

influencing factors that determine the early-age expansion and shrinkage development of the core concrete in nonstandard state; that is to say, the correction coefficients of various influencing factors such as the correction coefficients ($\alpha_{V/S}$) of volume-to-surface ratio of steel tubes, the types of concrete (α_{ck}), and active mineral additions (α_{fs}) should be taken into consideration. Therefore, the formula of multicoefficient model presented in this paper is clear in concept, convenient, and practical.

(2) Although the tests show that the strength of the concrete itself does not affect the expansion and shrinkage deformation, the factors that affect the above deformation such as cement content, different water-to-binder ratios, and aggregate condition are closely related to the concrete strength in varying degrees. So, the influence of these factors can be reflected indirectly and comprehensively by introducing the compressive strength of concrete. Therefore, the formula of ultimate shrinkage strain (ε_{shu}) of concrete under standard state contains 28 d average compressive strength parameter for its core concrete.

(3) Based on the analysis of shrinkage test of the core concrete pumped in steel tube in [20], the authors in this article hold that the parameters of component size such as volume-to-surface ratio (V/S) not only affect the development process ($\beta(t)$) of the expansion and shrinkage of CFST columns but also affect its final deformation values, especially the latter. So, the influence parameter on the V/S is included in the correction coefficient ($\alpha_{v/s}$) and the β parameter is included in the development function of shrinkage time ($\beta(t)$). In addition, the authors in this paper argue that, in the GL2000 model [21], the parameter of the volume-to-surface ratio has a greater impact on the time-development function when it is larger or smaller. Therefore, in view of the actual influence of the above parameters for CFST, the corresponding correction is made.

(4) In recent years, high-performance concrete (HPC) has been widely used in the core concrete of CFST. The obvious difference between HPC and ordinary concrete is that its composition has the fifth active mineral materials such as fly ash, silica fume, and slag. Therefore, in this model, there is correction coefficient (α_{fs}) of active mineral additions.

The formula is applicable to calculate expansion and shrinkage deformation of the core concrete in CFST. There is no reinforcement in the core concrete of steel tube. The time-development function of expansion and shrinkage is applicable for dimensions D ranging from 1000 mm to 1600 mm of CFST sections (D is the outer diameter of circular steel tube). The average compressive strength of the core concrete for 28 days is more than 60 MPa, and the value of water-to-binder ratio is less than 0.35; cement class is I, II, and III, as described as follows:

$$\varepsilon_{sh} = \beta(t) \cdot \varepsilon_{shu} \cdot \alpha_{V/S} \cdot \alpha_{ck} \cdot \alpha_{fs}, \quad (1)$$

where ε_{sh} refers to the expansion and shrinkage strain of the core concrete at age t; ε_{shu} is the ultimate shrinkage strain of the core concrete under standard conditions; $\beta(t)$ is the time-development function of expansion and shrinkage; $\alpha_{V/S}$ refers to the correction coefficient for volume-to-surface ratio; α_{ck} is the correction coefficient on the cement type; α_{fs} is the correction coefficient of active mineral addition.

The core concrete in CFST belongs to the massive concrete; that is, its section size is from 1000 mm to 1600 mm, and its time-development function is as follows:

$$\beta(t) = \frac{A_0 - 1}{1 + (t/\alpha)^{\beta}} + 1,$$

$$A_0 = \left\{ \begin{array}{ll} -0.0196 \times T + 0.9431 & \text{(vertical directions)} \\ -0.0358 \times T + 1.2176 & \text{(horizontal directions)} \end{array} \right\}, \quad (2)$$

where A_0 is the parameter of expansion strains, which is related to the temperature and expansion stress of the core concrete; α is the parameter of the turning point for the development between expansion and shrinkage strains, whose value is the day value in the horizontal coordinates, d; β is the trend and magnitude parameter of expansion and shrinkage strain, which is related to the section size of steel tube and the direction of vertical and horizontal expansion and shrinkage; t is the development time of the expansion and shrinkage age of the core concrete, d; β is the impact index of section size on the development of volume-to-surface ratio in the time-development function of expansion and shrinkage. The calculated results in terms of the abovementioned parameters are given in Tables 6–9.

The final shrinkage value (ε_{shu}) of plain concrete in formula (1) and the average compressive strength ($f_{cm,28}$) at 28 days can be used in view of the formula proposed by Gardner–Lockman model [21], as follows:

$$\varepsilon_{shu} = \left(\frac{30}{f_{cm,28}}\right)^{1/2} \cdot 10^{-3},$$

$$f_{cm,28} = 1.1 f_{ck} + 5\,(\text{MPa}). \quad (3)$$

Figure 9 gives the comparison of the calculation formula and test results. It can be seen from Figure 6 that the early-age expansion and shrinkage model of the massive self-compacting concrete pumped in steel tube columns is of better precision and applicability.

5. Discussion

Through shrinkage test, combined with hammering test of outer-wall of steel tube, inspection method of split damage test, and detection of cracks between the inner wall of steel tube and the core concrete by the electronic and visual crack observer, as shown in Figures 5(d) and 10, the following regularities of shrinkage cracks on the joint surface between

Table 6: The parameter values of time-development function for the early-age shrinkage and expansion.

Type of steel tube column	Expansion and shrinkage direction	Time-development function $\beta(t) = [(A_0 - 1)/(1 + (t/\alpha)^{\beta})] + 1(0 \le t)$				Curve mark
		A_0	α	β	Days of maximum expansion strains t_0	
SYZ-1	Vertical	−0.15	5.0	2.0	1.8	Model in Figure 9(a)
	Horizontal	−0.35	5.0	2.0	2.0	Model in Figure 9(a)
SYZ-2	Vertical	−0.06	4.5	1.5	0.4	Model in Figure 9(b)
	Horizontal	−0.30	4.5	1.5	1.2	Model in Figure 9(b)

It should be explained here that, before the day t_0 of the maximum expansion strains that can be achieved, the parameter A_0 is a variable; and then it is the constant value. According to the time $0 - t_0$ in Table 6, the parameter A_0 is interpolated linearly according to $0 - A_0$.

Table 7: The correction coefficient of volume-to-surface ratio of massive self-compacting concrete.

Type of steel tube column	The correction coefficient of volume-to-surface ratio $\alpha_{V/S}$	
	Vertical direction	Horizontal direction
SYZ-1	0.70	0.55
SYZ-2	0.52	0.45

Table 8: Influencing coefficient of substitution proportion of fly ash replacing cement [22].

Substitution proportion of fly ash replacing cement	0	10~20%	20~30%
α_{fs}	1	0.95	0.90

Table 9: Influencing coefficient of cement types on shrinkage [22].

Cement types	Ordinary or fast-hardening cement	Slow-hardening cement	Fast-hardening high-strength cement
α_{ck}	1.0	0.7	1.15

the inner wall of steel tube and the core concrete for massive self-compacting concrete pumped in steel tube column are summarized: the location of shrinkage cracks on the joint surface is "uncertain"; that is to say, the location of the above joint surface cannot be determined. The shrinkage cracks do not mean that as long as there is shrinkage deformation, there are shrinkage cracks on the joint surface of each location. The shrinkage deformation of different sections or different locations of the same section has "nonuniformity"; that is to say, the shrinkage size of different sections or different positions of the same section cannot be completely determined. The shrinkage crack size has "nonuniformity and uncertainty"; that is to say, the size of shrinkage crack for the joint surface cannot be accurately determined by the values of shrinkage deformation, but it can only be estimated roughly when the shrinkage cracks occur. The location of the shrinkage cracks is "symmetrical"; that is to say, the shrinkage cracks can sometimes occur at the same time on two relatively symmetrical planes. There is "uncertainty" between the above two, which cannot be accurately determined when the shrinkage cracks of the joint surface occur. Therefore, the shrinkage deformation of the core concrete must be strictly controlled to ensure structural safety.

6. Conclusions

Based on the experimental work and the analysis of the test results, the following conclusions can be drawn:

(1) The values of horizontal strains for early-age temperatures expansion are greater than those of the vertical ones. The two kinds of strains of the core concrete for small diameter CFST are greater than those of large diameter ones.

(2) The values of the vertical strains for early-age shrinkage are greater than those of the horizontal ones. The two kinds of strains of the core concrete for small diameter CFST are greater than those of large diameter ones.

(3) The shrinkage deformation of the core concrete in CFST develops rapidly in the early stage, and the values of its horizontal shrinkage are slightly less

(a) (b)

Figure 10: Detection of cracks between steel tube wall and the core concrete. (a) Detecting by electronic crack observer. (b) Detecting by visual crack observer.

than those of the vertical ones at the same time. But the deformation rates show a decreasing trend with the increase of time. After 28 days, the shrinkage deformation curves in this paper become horizontal gradually.

(4) The change of section size and volume-to-surface ratio has a great influence on shrinkage deformation of the core concrete. With the increase of section size, the shrinkage deformation values of the core concrete decrease. The influence of volume-to-surface ratio of CFST should be reasonably considered in calculating shrinkage deformation of the core concrete.

(5) The calculation model for the early-age shrinkage and expansion is proposed for the massive self-compacting concrete pumped in steel tube column.

Data Availability

All data, models, or codes generated or used in this paper are available from the corresponding author upon request.

Conflicts of Interest

The authors declare that they have no conflicts of interest.

Acknowledgments

This study was funded by the Yuyou Talent Support Plan of the North China University of Technology (Grant no. 2018-39).

References

[1] Y. F. Yang, L. H. Han, and X. Wu, "Concrete shrinkage and creep in recycled aggregate concrete-filled steel tubes," *Advances in Structural Engineering*, vol. 11, no. 4, pp. 383–396, 2008.

[2] J. M. Abdalhmid, A. F. Ashour, and T. Sheehan, "Long-term drying shrinkage of self-compacting concrete: experimental and analytical investigations," *Construction and Building Materials*, vol. 202, no. 2, pp. 825–837, 2019.

[3] P. Y. Yan, F. Zheng, J. Peng et al., "Relationship between delayed ettringite formation and delayed expansion in massive shrinkage-compensating concrete," *Cement and Concrete Composites*, vol. 26, no. 6, pp. 383–396, 2004.

[4] A. Gonzalez-Corominas and M. Etxeberria, "Effects of using recycled concrete aggregates on the shrinkage of high performance concrete," *Construction and Building Materials*, vol. 115, no. 4, pp. 32–41, 2016.

[5] M. J. Oliveira, A. B. Ribeiro, and F. G. Branco, "Curing effect in the shrinkage of a lower strength self-compacting concrete," *Construction and Building Materials*, vol. 93, no. 4, pp. 1206–1215, 2015.

[6] V. Gribniak, G. Kaklauskas, R. Kliukas, and R. Jakubovskis, "Shrinkage effect on short-term deformation behavior of reinforced concrete-when it should not be neglected," *Materials & Design*, vol. 51, no. 9, pp. 1060–1070, 2013.

[7] D. Shen, J. Jiang, J. Shen, P. Yao, and G. Jiang, "Influence of curing temperature on autogenous shrinkage and cracking resistance of high-performance concrete at an early age," *Construction and Building Materials*, vol. 103, no. 1, pp. 67–76, 2016.

[8] A. Wendling, K. Sadhasivam, and R. W. Floyd, "Creep and shrinkage of lightweight self-consolidating concrete for prestressed members," *Construction and Building Materials*, vol. 167, no. 2, pp. 205–215, 2018.

[9] F. Benboudjema, F. Meftah, and J. M. Torrenti, "Interaction between drying, shrinkage, creep and cracking phenomena in concrete," *Engineering Structures*, vol. 27, no. 2, pp. 239–250, 2005.

[10] L. Wu, N. Farzadnia, C. Shi, Z. Zhang, and H. Wang, "Autogenous shrinkage of high performance concrete: a review," *Construction and Building Materials*, vol. 149, no. 5, pp. 62–75, 2017.

[11] B. Persson, "Experimental studies on shrinkage of high-performance concrete," *Cement and Concrete Research*, vol. 28, no. 7, pp. 1023–1036, 1998.

[12] T. Xie, C. Fang, M. S. Mohamad Ali, and P. Visintin, "Characterizations of autogenous and drying shrinkage of ultra-high performance concrete (UHPC): an experimental study," *Cement and Concrete Composites*, vol. 91, no. 4, pp. 156–173, 2018.

[13] X. F. Wang, C. Fang, W. Q. Kuang, D. W. Li, N. X. Han, and F. Xing, "Experimental investigation on the compressive strength and shrinkage of concrete with pre-wetted lightweight aggregates," *Construction and Building Materials*, vol. 155, no. 6, pp. 867–879, 2017.

[14] M. J. Oliveira, A. B. Ribeiro, and F. G. Branco, "Combined effect of expansive and shrinkage reducing admixtures to control autogenous shrinkage in self-compacting concrete,"

Construction and Building Materials, vol. 52, no. 1, pp. 267–275, 2014.

[15] S. Ribeiro, A. Z. Bendimerad, E. Rozière, and A. Loukili, "How do recycled concrete aggregates modify the shrinkage and self-healing properties?" *Cement and Concrete Composites*, vol. 86, no. 1, pp. 72–86, 2018.

[16] B. C. Chen and Y. Lai, "Shrinkage deformation of concrete filled steel tube and shrinkage stress of concrete filled steel tubular arch," *Journal of Railway*, vol. 38, no. 2, pp. 112–123, 2016.

[17] G. H. Cao, K. Zhang, J. X. Hu et al., "Calculation model of shrinkage for expansive concrete filled steel tube," *Journal of Central South University (Science and Technology)*, vol. 46, no. 3, pp. 1094–1099, 2015.

[18] H. B. Zhu, Q. S. Yuan, J. Xiang et al., "Experimental research on expansive performance of micro-expansive lightweight aggregate concrete filled steel tube," *Sichuan Building Science*, vol. 43, no. 3, pp. 135–138, 2017.

[19] W. X. Chen, "Research on shrinkage and crack resistance performance of self-compacting concrete for underwater steel pipe columns of shanghai-nantong yangtze river bridge," *Railway Engineering*, vol. 58, no. 12, pp. 150–155, 2018.

[20] L. H. Han, *Concrete Filled Steel Tube Structure-Theory and Practice*, Science Press, Beijing, China, 2007.

[21] N. J. Gardner and M. J. Lockman, "Design provisions for drying shrinkage and creep of normal-strength concrete," *ACI Materials Journal*, vol. 98, no. 2, pp. 159–167, 2001.

[22] L. S. Gong, M. Y. Hui, B. Yang et al., "Experimental study on shrinkage and creep of concrete," *Report on Architectural Science Research*, China Academy of Building Research, Beijing, China, 1987.